Electrochimica Acta 130 (2014) 387–396

Contents lists available at ScienceDirect

Electrochimica Acta

journal homepage: www.elsevier.com/locate/electacta

Investigation on PCET–accompanied Dimerization of 5–hydroxy–1, 4–naphthoquinone in the Process of Electrochemical Reduction by In Situ FT–IR Spectroelectrochemistry and Density Functional Calculation

Dan Li, Longjiu Cheng, Baokang Jin*

Department of Chemistry, Anhui University, Hefei 230039, People's Republic of China

ARTICLE INFO

Article history:
Received 13 December 2013
Received in revised form 9 March 2014
Accepted 9 March 2014
Available online 22 March 2014

Keywords:
dimerization
proton coupled electron transfers (PCET)
5–hydroxy–1, 4–naphthoquinone
hydrogen–bonding
in situ FT–IR spectroelectrochemistry
density functional calculation

ABSTRACT

Electron transfers (ET) of 5–hydroxy–1, 4–naphthoquinone (HNQ) and 5–hydroxy–2–methyl–1, 4–naphthoquinone (HMeNQ) have been investigated in acetonitrile and proton donors mixed media. Although there is merely a small difference in structure between HMeNQ, having a methyl, and HNQ, not having a methyl, the reduction of HNQ involves proton coupled electron transfers (PCET) process while HMeNQ not. Both CV and rapid–scan IR spectra support the existence of intermediate $HNQ^{\bullet -}$ and dimer in acetonitrile during electrochemical reduction. Density functional calculations show that proton transfers (PT) occur when forming dimer, indicating that HNQ has PCET–accompanied dimerization mechanism. Besides, dimer also undergoes two successive ET processes to form quinone. When proton donors are added to HNQ, dimerization is inhibited owing to intermolecular hydrogen–bonding, accompanying by the interruption of PCET process.

1. Introduction

Quinones are of biological significance in function owing to their contribution on electron transfer in biology.[1–5] The mechanism of electrochemical reduction of quinones has been studied extensively.[6–11] Quinones are known to undergo two–step one–electron process in aprotic solvents, forming a radical anion intermediate in the first step and the dianion in the second step accordingly. Dimerization is one of the important organic radical reactions.[12–14] Anion radicals of certain quinones like 2, 3–dichloro–5, 6–dicyano–1, 4–benzoquinone really undergo interaction to form dimers.[15] Hydroxyquinones can easily form intramolecular hydrogen–bonding owing to hydroxyl.[16,17] In addition, the electrochemical reductions of hydroxyquinones show that hydroxyquinones could easily undergo the dimerization to form neutral–anion radical complex owing to hydrogen–bonding.[18] While 5–hydroxy–1, 4–naphthoquinone (HNQ) represents a special case in acetonitrile, anion–anion radical dimer forming instead of neutral–anion radical complex.[19] Proton–coupled electron transfers (PCET), where proton and electron transfer involves different molecular, has a long experimental and theoretical history.[4,5,20–26] Such reactions can occur by means of either concerted or stepwise mechanisms. Although dimerization has received great attention, very little is known about PCET-accompanied dimerization and the inhibition of dimerization by intermolecular hydrogen–bonding.

In this study, the electron transfer of HNQ and 5–hydroxy–2–methyl–1, 4–naphthoquinone (HMeNQ) in aprotic and proton donors mixed media were investigated by in situ FT–IR spectroelectrochemistry, cyclic voltabsorptometry (CVA) and derivative cyclic voltabsorptometry (DCVA).[8,27] The results come from cyclic voltammetry (CV), IR spectroelectrochemistry, and density functional calculations, indicating PCET–accompanied dimerization mechanism for HNQ. In addition, intermolecular hydrogen–bonding can block PCET process and dimerization.

The structures of HMeNQ and HNQ are listed in Scheme 1.

2. Experimental Section

2.1. Chemicals

5–hydroxy–1, 4–naphthoquinone (Sigma–Aldrich, 97%), 5–hydroxy–2–methyl–1, 4–naphthoquinone (Sigma–Aldrich) and acetonitrile (Sigma–Aldrich, HPLC) were used as received.

* Corresponding author.
E-mail addresses: bkjinhf@aliyun.com, echem@ahu.edu.cn (B. Jin).

http://dx.doi.org/10.1016/j.electacta.2014.03.049
0013-4686/

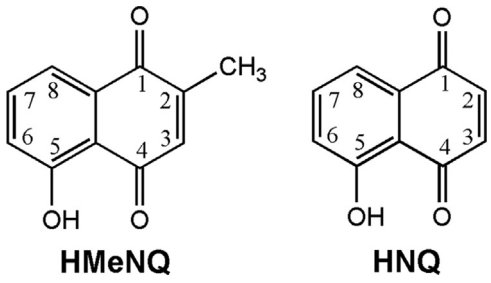

Scheme 1. Structure of HMeNQ and HNQ.

Tetrabutylammonium perchlorate (Et_4NBF_4) was recrystallized twice and dried at 100 °C for 24 h before use. The solution was degassed with nitrogen for 10 min before experiment.

2.2. Voltammetry

The electrochemistry apparatus was electrochemical analyzer CHI630 potentiostat. The thin–layer was made by ourselves as a spectroelectrochemical cell.[28] A 4 mm gold disk was used as a working electrode, a Ag/AgCl as the reference electrode and a Pt as an auxiliary electrode. The working electrode was polished with 0.05 μm α–alumina slurry, rinsed thoroughly with double distilled water. Finally ultrasonic cleaner was used to clear it for 10 min.

2.3. In Situ FT–IR Spectroelectrochemistry

In situ FT–IR spectroelectrochemistry apparatus was Nicolet Nexus 870 spectromter which was equipped with a specular reflectance accessory and a HgCdTe/A detector cooled with liquid-nitrogen. Each spectrum was made up of 25–60 interferograms. The sampling interval was 0.7–1.8 s. The resolution was 16 cm^{-1}. In situ FT–IR experiments were carried out with electrochemistry experiments happening simultaneously.

2.4. Theoretical computation

The anion radical and possible structures were relaxed at the B3LYP/6-311++G** level of theory with the solvent effects. All theoretical calculations were carried out by the Gaussian 09 package.[29] The value in the brackets was relative energy in eV.

3. Results and Discussion

3.1. HMeNQ in aprotic media (CH3CN)

As shown in Fig. 1A, reduction of HMeNQ was carried out in acetonitrile. Two well–defined couples of anodic and cathodic peaks are observed, with potential values $^1E_{1/2}$= -0.557 V and $^2E_{1/2}$= -0.975 V (defined as $E_{1/2}=(E_{pa}+E_{pc})/2$).

The rapid–scan IR spectra recorded in situ during the CV scan of HMeNQ are shown in Fig. 1B. The 3D spectra were gathered during the scan between -0.2 V and -1.4 V. The spectrum recorded at -0.2 V was used as the reference spectrum. Three types of IR peaks are observed. The first type, including two distinct upward peaks at 1510 cm^{-1} and 1310 cm^{-1}, is assigned to $\nu_{C=C}$ and ν_{C-O} of the anion radical ($HMeNQ^{\bullet-}$). The second type, including three distinct upward peaks at 1387 cm^{-1}, 1356 cm^{-1} and 1214 cm^{-1}, is assigned to ν_{C-O} of the final reduced product dianion ($HMeNQ^{2-}$). The third is two downward peaks at 1649 cm^{-1} and 1256 cm^{-1}, which are assigned to $\nu_{C=O}$ and other group vibration of quinone (HMeNQ).[8,27] All these peaks can be employed to track the corresponding species concentration during the electrochemical reactions.

In order to further explore IR absorption behavior, the rapid-scan IR spectra are operated to CVA (Fig. 2A). The peaks at 1649, 1510 and 1387 cm^{-1} are selected as band representatives to track the concentration change of HMeNQ, $HMeNQ^{\bullet-}$ and $HMeNQ^{2-}$. There is a periodic increase and decrease of absorbance at 1649, 1510 and 1387 cm^{-1} with the sweep potential (time), corresponding to the reduction from HMeNQ to intermediate $HMeNQ^{\bullet-}$, and $HMeNQ^{\bullet-}$ is further reduced to $HMeNQ^{2-}$.

It has been demonstrated that dA/dt (or dA/dE) versus E is morphologically identical to a cyclic voltammogram.[30] It is apparent from Fig. 2B that the shape of DCVA at 1510 cm^{-1} corresponding to $HMeNQ^{\bullet-}$ is similar to that of CV shown in Fig. 1A, where two redox couples of peaks are observed. DCVA couple of the absorbance at 1649 cm^{-1} corresponds to the redox couple of $HMeNQ/HMeNQ^{\bullet-}$ (the first electrochemical step). DCVA couple of the absorbance at 1387 cm^{-1} corresponds to the redox couple of $HMeNQ^{\bullet-}/HMeNQ^{2-}$ (the second electrochemical step). Thus both the results of CVA and DCVA show that HMeNQ undergoes two successive ET processes.

3.2. HMeNQ in proton donors mixed media

It is well known that the radical anion and dianion are hydrogen–bonding acceptors.[31,32] In order to study the affect of hydrogen–bonding donors on the electrochemical reduction of HMeNQ, ethanol was selected as a proton donor (Fig. 3). As shown in Fig. 3A, adding C_2H_5OH to acetonitrile results in redox potential of HMeNQ positive shifts. For given proton donor concentration, the shift is much larger for the second one.

In situ FT–IR spectroelectrochemistry can help us understand the behavior of hydrogen–bonding during electrochemical process. The 3D spectra of HMeNQ in CH_3CN with 10% C_2H_5OH (Fig. 3B) are recorded. A series of bands at 1649, 1387, 1510 cm^{-1} is depicted

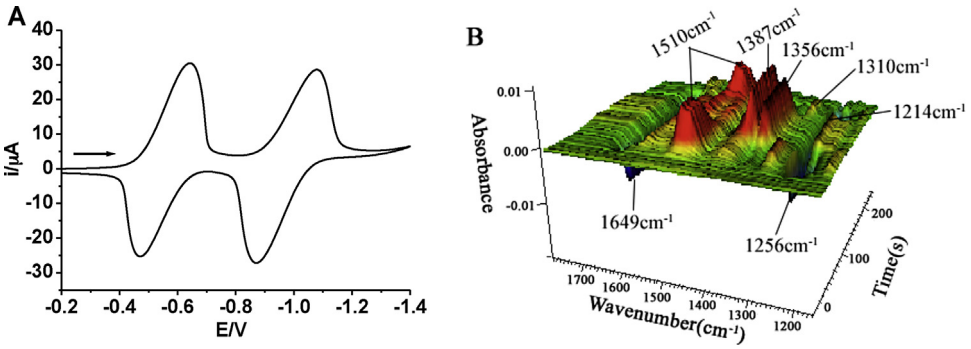

Fig. 1. Cyclic voltammogram (A) and the corresponding 3D spectra (B) in acetonitrile containing 10 mM HMeNQ and 0.2 M Bu_4NClO_4 as the supporting electrolyte. The potential scan rate was 10 mVs^{-1}.

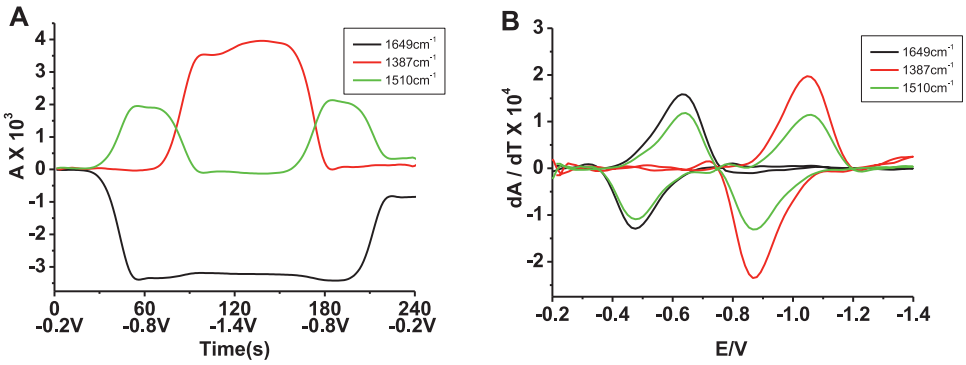

Fig. 2. CVA (A) and DCVA (B) for HMeNQ at 1649, 1387, 1510 cm^{-1}. To make the DCVA data readily comparable to CV, the DCVA data of 1649 cm^{-1} were multiplied by -1, and 1510 cm^{-1} in the second reduction and the first oxidation were multiplied by -1.

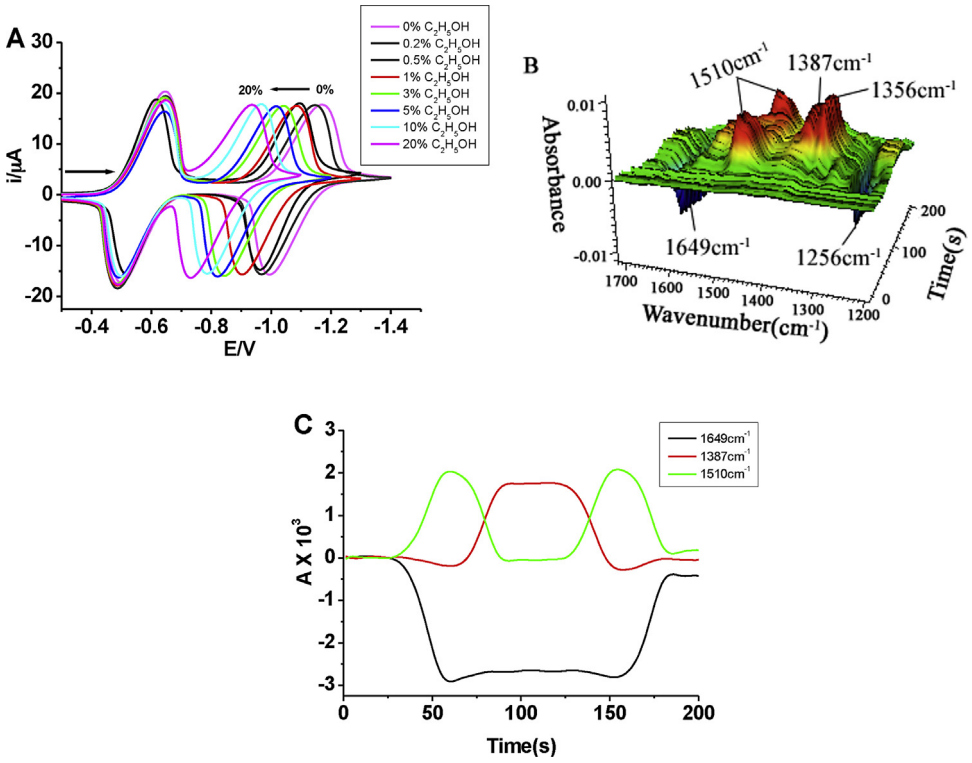

Fig. 3. Cyclic voltammograms (A) and the corresponding 3D spectra (B) in CH_3CN+ C_2H_5OH (10%) proton donors mixed media and CVA (C) containing 10 mM HMeNQ and 0.2 M Bu_4NClO_4 as the supporting electrolyte. The potential scan rate was 10 mVs^{-1}.

in Fig. 3C. It is worth mentioning that the lifttime of intermediate existence C_2H_5OH is shorter than that in acetonitrile. The above results suggest that hydrogen–bonding occurs between proton donors and the electrochemical products $HMeNQ^{\bullet-}$/$HMeNQ^{2-}$.

The electrochemical reduction of HMeNQ in acetonitrile and ethanol mixed media can be expatiated as:

$$HMeNQ + e + mC_2H_5OH \leftrightharpoons HMeNQ^{\bullet-}\cdots(C_2H_5OH)_m \quad (1)$$

$$HMeNQ^{\bullet-}\cdots(C_2H_5OH)_m + e + (n\text{-}m)C_2H_5OH \leftrightharpoons HMeNQ^{2-}\cdots(C_2H_5OH)_n \quad (2)$$

Where m and n are the number of molecule of proton donor hydrogen–bonded to $HMeNQ^{\bullet-}$ and $HMeNQ^{2-}$, respectively. And "…" represents hydrogen–bonding. Values of m and n can be obtained by the following equation:

$$E_{1/2} = E^0_{1/2} + (RT/F)\ln(1 + K_{eq}[C_2H_5OH]^n) \quad (3)$$

Where $E^0{}_{1/2}$ is the half–wave potential of HMeNQ in the aprotic media. $E_{1/2}$ is the half–wave potential in the proton donors mixed media. R is the universal gas constant. T is the absolute temperature. F is Faraday's constant. On $K_{eq}[C_2H_2OH]^n \gg 1$, a plot of $\Delta E_{1/2}$ vs $\lg[C_2H_2OH]$ should give a straight line with a slope of 2.3nRT/F. A straight line with a slope 0.114 in Fig. 4 can be found. It can be obtained that one $HMeNQ^{2-}$ molecular combines with about 1.9 C_2H_5OH molecular to form hydrogen–bonding.

3.3. HNQ in aprotic media (CH_3CN)

Typical CV of HNQ with slow scan rate shows two well–defined couples of anodic and cathodic peaks, with potential values being $^1E_{1/2}$= -0.518 V and $^2E_{1/2}$= -0.993 V (Fig. 5A). Current values of A_1 and C_1 are much larger than A_2 and C_2. When the potential value reaches E= -0.137 V in the oxidation process, an anodic peak A_4 is observed. There is a weak anodic peak A_3 between A_2 and A_4. The potential value of A_3 is about 0.32 V. Potential difference between

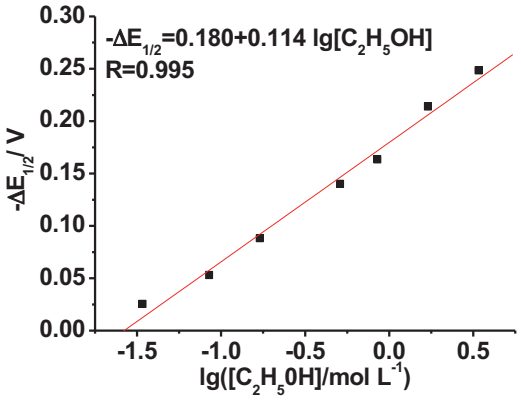

Fig. 4. Plot of $-\Delta E_{1/2}$ (= - ($E_{1/2}$- $E^0{}_{1/2}$)) for HMeNQ vs lg ([C_2H_5OH]/mol L^{-1}) at different concentrations of C_2H_5OH in CH_3CN respectively.

A_3 and A_4 is 0.173 V. Fig. 5C shows the CV of HNQ on the condition of semi–infinite diffusion with scan rate at 80 mVs^{-1}.

It should be stated that our in situ FT–IR spectroelectrochemistry experiments are developed in a thin–layer cell, with slow potential scan rate. CV of HNQ on the condition of semi–infinite diffusion (Fig. 5C) is similar to that of literature.[19] Why the shape of CV changes when potential scan rate is slow? A reasonable hypothesis is that slow chemical reactions are coupled with the electrochemical process. As shown in Fig. 5B, there are also three types of IR peaks corresponding to two successive ET processes. In addition, upward peak in other form like 1618 cm^{-1} is observed.

The rapid–scan IR spectra are further operated to CVA (Fig. 6A). Absorbance at 1641 cm^{-1} doesn't return to the initial value when all the experiment is over.[18] It has a significant gap, compared with absorbance at 1649 cm^{-1} of HMeNQ. The result strongly supports the existence of chemical reactions like dimerization as previously suggested for HNQ by Macias-Ruvalcaba and Evans.[19] The variation of peak at 1618 cm^{-1} in Fig. 6A is similar to that of peak at 1525 cm^{-1}, undergoing the process of increasing firstly, then decreasing in the reduction process. Then the same process repeats in the oxidation process. However, the absorbance at 1618 cm^{-1} starts to increase for the third time at -0.32 V (268s). And it reaches its maximum at -0.06 V (294s). Thus absorbance at 1618 cm^{-1} can be assigned to vibration of $HNQ^{\bullet-}$. And $HNQ^{\bullet-}$ reacts to convert to another new species which has a similar structure as $HNQ^{\bullet-}$. The new species begin to be oxidized at -0.32 V (268s). It is very likely that the new species is dimer.

The shape of DCVA (Fig. 6B) at 1618 cm^{-1} has the similar shape as CV shown in Fig. 5A, where two redox couples of peaks and peak A_4 can be observed. It is found that no new IR band appears or disappears. Only the intensity of band (1618 cm^{-1}) varies when peak A_4 appears. The dimer which has similar structure to $HNQ^{\bullet-}$ can lead to changes in intensity of band without new IR band appearing or not.

In order to further explore the relationship between peak A_4 and dimer, we shorten the scan range to 0.2~ -0.8 V (Fig. 7A). Peak A_4 still appears despite the inexistence of peaks C_2/A_2. It is obvious that peak A_4 just relates to C_1/A_1, which correspond to the reduction process from HNQ to $HNQ^{\bullet-}$. As shown in Fig. 7C, absorbance at 1618 cm^{-1} increases once again at nearly -0.35 V (145s) and starts to decrease again at -0.04 V (176s). DCVA at 1618 cm^{-1} (Fig. 7D) is similar to CV shown in Fig. 7A, where one redox couple of peaks, corresponding to the redox couple HNQ/$HNQ^{\bullet-}$, and peak A_4 can be observed. Similarly, no new IR band appears or disappears, only the intensity of band (1618 cm^{-1}) varies when peak A_4 appears in DCVA. Since peak A_4 just relates to the reduction process from HNQ to $HNQ^{\bullet-}$, we confirm that $HNQ^{\bullet-}$ which can be tracked by absorbance at 1618 cm^{-1} convert to dimer which has the similar structure as $HNQ^{\bullet-}$. The dimer begins to be oxidized at -0.35 V (145s).

CV under consecutive scan (Fig. 8A) and the corresponding 3D spectra (Fig. 8B) with scan range from 0.2 to -0.8 V were conducted. When potential reaches E= -0.171 V, a cathodic peak C_4, corresponding to A_4, appears in the second and third scan. Similarly, a weak cathodic peak C_3, corresponding to A_3, appears in the second

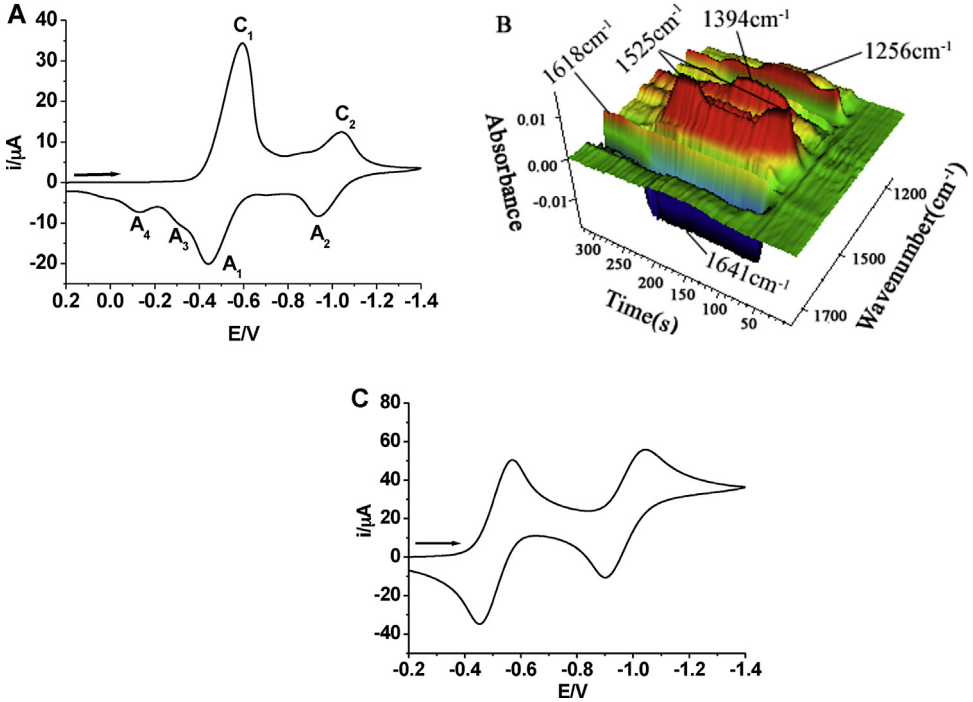

Fig. 5. Cyclic voltammogram (A) and the corresponding 3D spectra (B) in acetonitrile containing 10 mM HNQ and 0.2 M Bu_4NClO_4 as the supporting electrolyte. The potential scan rate was 10 mV s^{-1}. Cyclic voltammogram (C) in acetonitrile containing 2 mM HNQ and 0.1 M Bu_4NClO_4 as the supporting electrolyte, potential scan rate 80 mVs^{-1}.

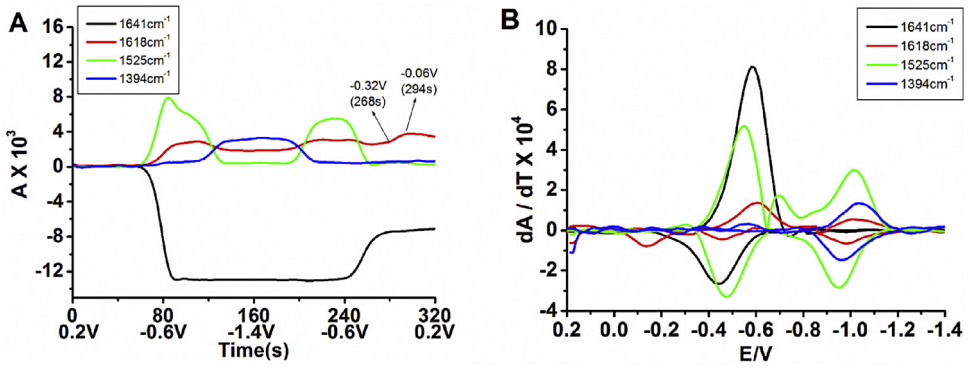

Fig. 6. CVA (A) and DCVA (B) for HNQ at the four IR absorption peaks in acetonitrile. To make the DCVA data readily comparable to CV, the DCVA data of 1641 cm^{-1} were multiplied by -1, and 1525 cm^{-1} and 1618 cm^{-1} in the second reduction and the first oxidation were multiplied by -1, and 1618 cm^{-1} in the third oxidation were multiplied by -1.

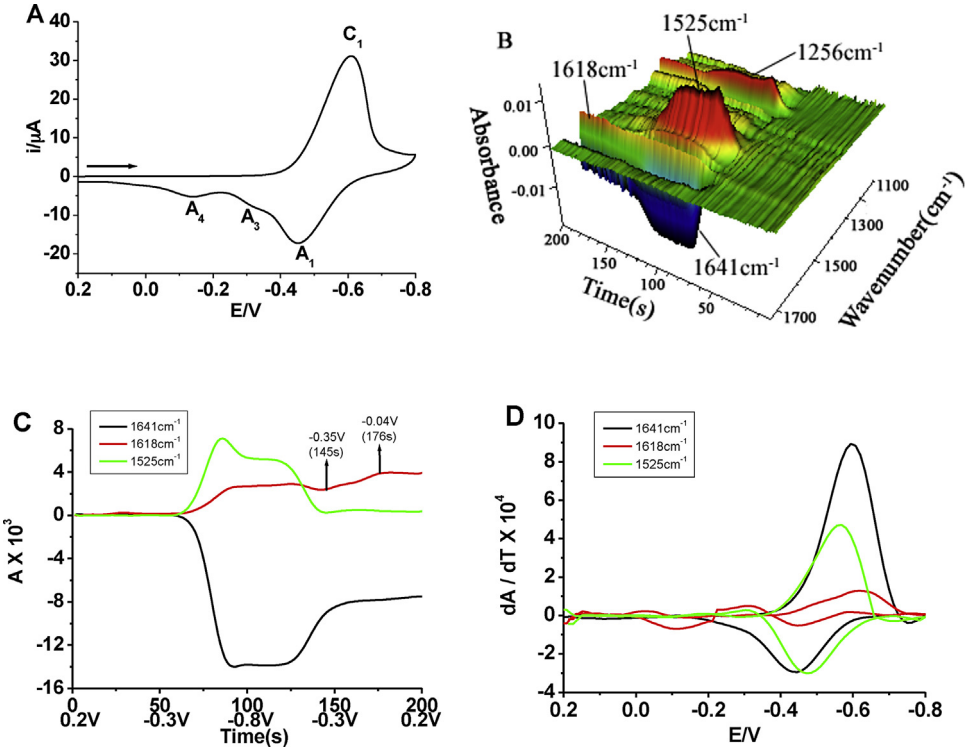

Fig. 7. Cyclic voltammogram (A) and the corresponding 3D spectra (B) in acetonitrile containing 10 mM HNQ and 0.2 M Bu_4NClO_4 as the supporting electrolyte. The potential scan rate was 10 mVs^{-1}. CVA (C) and DCVA (D) for HNQ at the three IR absorption peaks in acetonitrile. To make the DCVA data readily comparable to CV, the DCVA data of 1641 cm^{-1} were multiplied by -1, and 1618 cm^{-1} in the second oxidation were multiplied by -1.

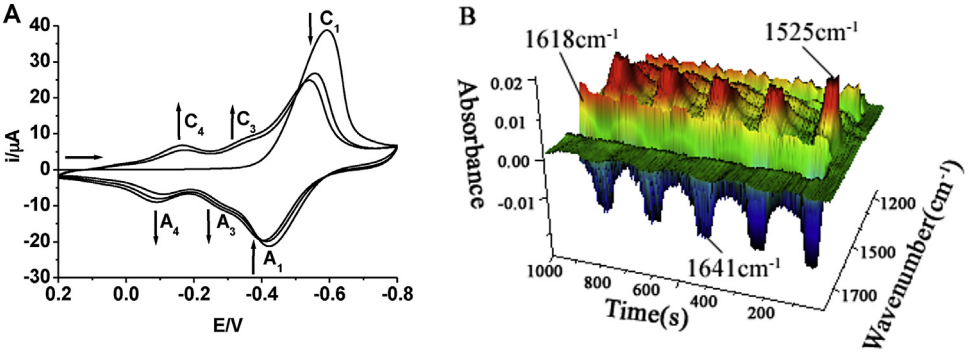

Fig. 8. Continuous Cyclic voltammogram (A) and the corresponding 3D spectra (B) in acetonitrile containing 10 mM HNQ and 0.2 M Bu_4NClO_4 as the supporting electrolyte. The potential scan rate was 10 mVs^{-1}.

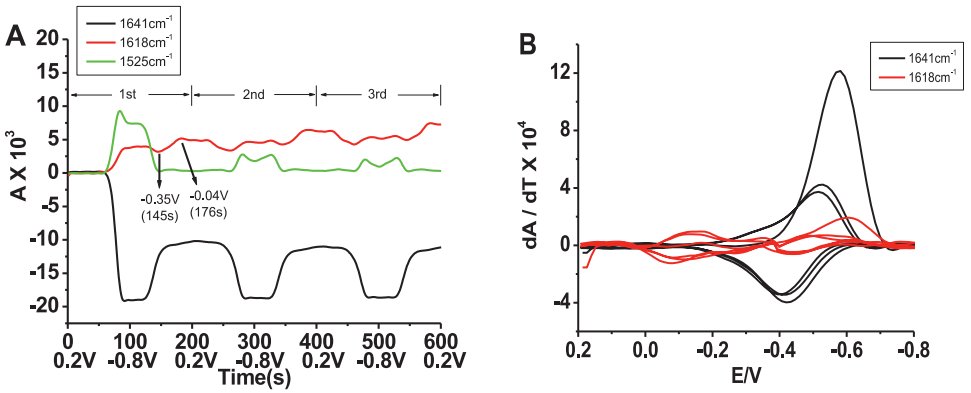

Fig. 9. CVA (A) at the three IR absorption peaks and DCVA (B) at the two IR absorption peaks for HNQ in acetonitrile. To make the DCVA data readily comparable to CV, the DCVA data of 1641 cm^{-1} were multiplied by -1, and 1618 cm^{-1} in the second oxidation in all the three cycle and the second reduction in the last two cycle were multiplied by -1.

and third scan. Current values of peak C_1/A_1 decrease while values of other peaks increase with added scan circles. As shown in Fig. 8B, absorbance at 1618 cm^{-1} increases continuously in the whole process, indicating chemical reactions happening together with the electrochemical reactions. Current value of C_4/A_4 is higher than that of C_3/A_3. For most quinone current value of the first reduction step is higher than the second.[11] So we suppose that the dimer be further oxidized, undergoing two successive ET process to form quinone.

It can be observed more directly from CVA in Fig. 8A. In the first scan absorbance at 1618 cm^{-1} increases once again at -0.35 V (145s). Then it reaches its maximum at -0.04 V (176s). Next it starts to decrease slightly. In the second and third scan, the same processes repeat as the first scan. The band at 1641 cm^{-1} doesn't return to the initial value when all the experiments are over. It shows that chemical reactions happen together with the electrochemical reactions.

The shape of DCVA at 1618 cm^{-1} (Fig. 9B) has the couple of the anodic and cathodic peaks at -0.1 ~ -0.2 V corresponding to A_4 and C_4 in Fig. 8A. We conclude that it is dimer $(HNQ)_2^{2-}$ which has the similar structure with anion radical that loses/gets electron at -0.1 ~ -0.2 V.

3.4. HNQ in proton donors mixed media

Experiments of HNQ in proton donor mixed media are also developed. As shown in Fig. 10A, peak current values of A_2 and C_2 increase, while A_4 and A_3 first decrease and then vanish when concentrations of C_2H_5OH are increased. Variation related to dimer in CVA (Fig. 10C) and DCVA (Fig. 10D) also vanishes when a certain

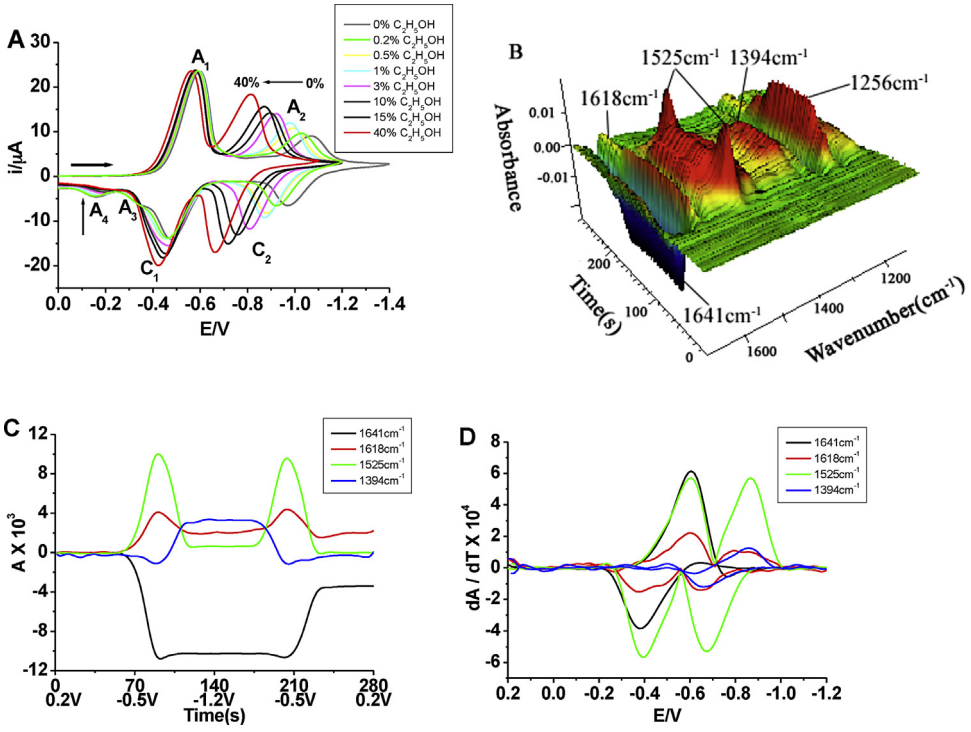

Fig. 10. Cyclic voltammograms (A) and the corresponding 3D spectra (B) in CH_3CN+ C_2H_5OH (20%) mixed media containing 10 mM HNQ and 0.2 M Bu_4NClO_4 as the supporting electrolyte. The potential scan rate was 10 mVs^{-1}. CVA (C) and DCVA (D) at the four IR absorption peaks in acetonitrile. To make the DCVA data readily comparable to CV, the DCVA data of 1641 cm^{-1} were multiplied by -1, and 1525 cm^{-1} and 1618 cm^{-1} in the second reduction and the first oxidation were multiplied by -1, and 1618 cm^{-1} in the third oxidation were multiplied by -1.

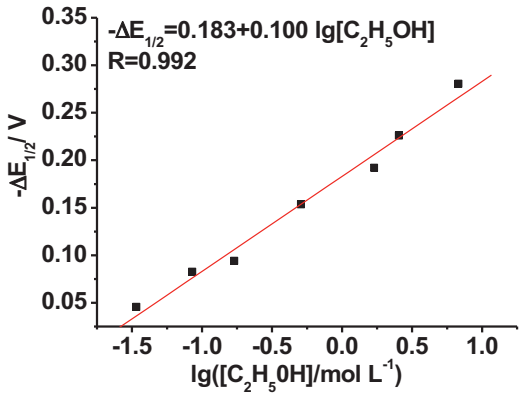

Fig. 11. Plot of $-\Delta E_{1/2}$ (= - ($E_{1/2}$ - $E^0{}_{1/2}$)) for HNQ vs lg [C_2H_5OH]/molL^{-1} at different concentrations of C_2H_5OH in CH_3CN respectively.

proportion proton donor is added. All these imply the inhibition of conversion from anion radical to dimer when proton donor is added. In addition, the inhibition intensifies with the concentration of proton donor increasing. It is probable that hydrogen–bonding between proton donor and $HNQ^{\bullet-}$ causes the inhibition.

Similarly, the electrochemical reduction of HNQ in acetonitrile and ethanol mixed media can be expatiated as:

$$HNQ + e + mC_2H_5OH \leftrightharpoons HNQ^{\bullet-}\cdots(C_2H_5OH)_m \quad (4)$$

$$HNQ^{\bullet-}\cdots(C_2H_5OH)_m + e + (n\text{-}m)C_2H_5OH \leftrightharpoons HNQ^{2-}\cdots(C_2H_5OH)_n \quad (5)$$

A straight line with a slope 0.100 in Fig. 11 can be found. It can be obtained that one HNQ^{2-} molecular combines with about 1.7 C_2H_5OH molecular to form hydrogen–bonding.

3.5. Theoretical computation

The energy of anion radical and possible dimer structures are calculated and the results are listed in Fig. 12. For HNQ, the energy of dimer 1 and dimer 2 is relative energy to $HNQ^{\bullet-}$. So the energy of $HNQ^{\bullet-}$ is confirmed as 0.00 eV. It is same for HMeNQ. Here only the global minima are given (other lower-energy structures are provided in the supporting information). The corresponding structures are listed in Scheme 2.

We have calculated three kinds of anion–anion radical dimer–C–centered and C–centered, C–centered and O–centered, and O–centered and O–centered radical dimer respectively. Besides, density functional calculation shows that neutral–anion radical dimer doesn't exist.[19]

In Fig. 12 the distance between O (5–, numbered in Scheme 2) and H is 0.98 Å. The distance between O (4–) and H is 2.16 Å. So O (4–) and H are joined by hydrogen bonds while O (5–) and H are joined by covalent bond. Dimer 1 is the lowest in energy (0.63 eV) among C–centered and C–centered radical dimer. And dimer 2 is the lowest in energy (0.23 eV) among C–centered and O–centered radical dimer. Besides, dimerization between O–centered and O–centered doesn't exist. It is very interesting for dimer 1 that the distance between O (4–) and H shorten to 1.02 Å, while the distance between O (5–) and H lengthen to 1.51 Å. So H transfers from O (5–) to O (4–) during the formation of dimer 1. All these can be observed more straightforward in Scheme 2. It indicates a proton transfer process. Homologous phenomenon of proton transfers is observed for dimer 2, H transfering from O (5–) to O (4–). In addition, H transfers from C (2–) to O of carbonyl (1–) in C-centered fragment. Dimer 2 is 0.40 eV lower than dimer 1. So dimer 2 is the most stable dimer structure. In the forming process of dimer 2, electron transfer (ET) occurs when froming intermediate $HNQ^{\bullet-}$; then proton transfer (PT) occurs when forming dimer 2 (Scheme 3). So, reactions occur by stepwise pathways in which both electron and proton transfer but are separated. ET is followed by PT.

For HMeNQ, dimers are much higher (1.47 eV, 0.97 eV) in energy than that of anion radical. So dimers are difficult to form. It is probably a steric effect of methyl that leads to inhibition of dimerization.

Although there is merely a small difference in structure between HMeNQ, having a methyl, and HNQ, not having a methyl, the reduction of HNQ involves proton coupled electron transfers (PCET) process while HMeNQ not.

As discussed in CV experiments, we suppose that dimer 2 of HNQ be further oxidized to radical anion in the first step and quinone in

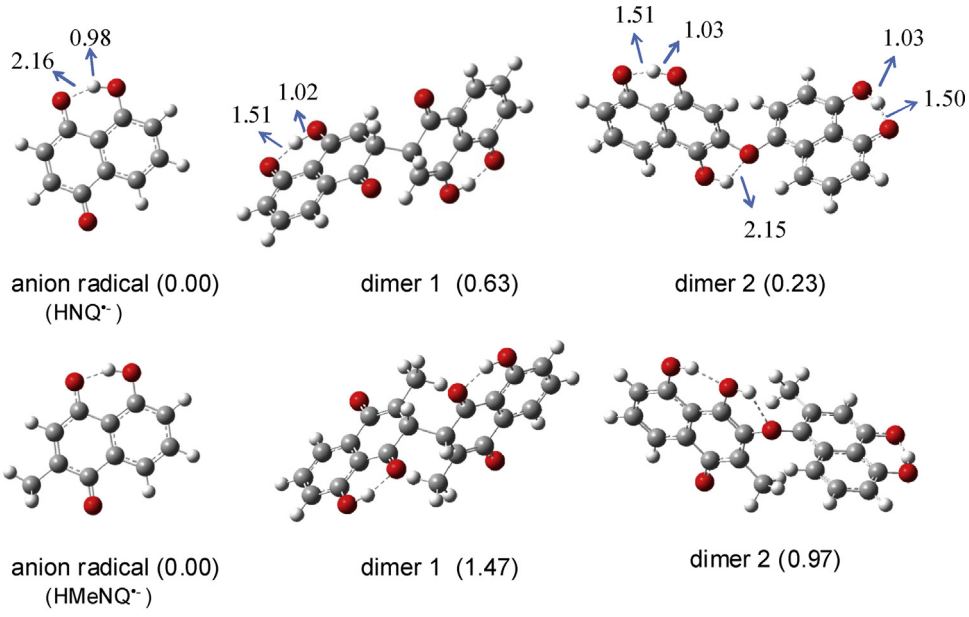

Fig. 12. The monomer and low–energy isomers for dimer at B3LYP/6-311++G** level. The value in the brackets is relative energy in eV.

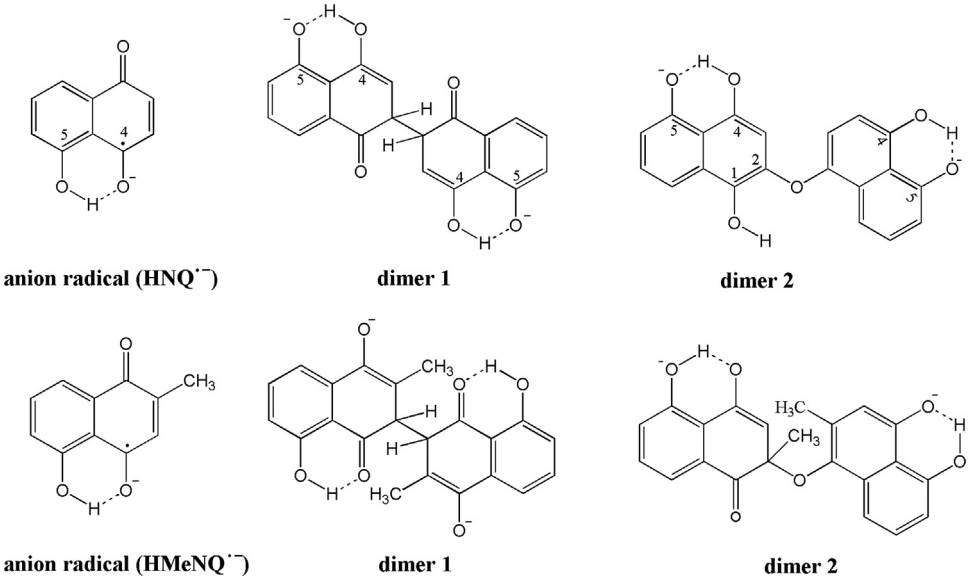

Scheme 2. Possible structures of anion radical and dimer corresponding to Fig. 12.

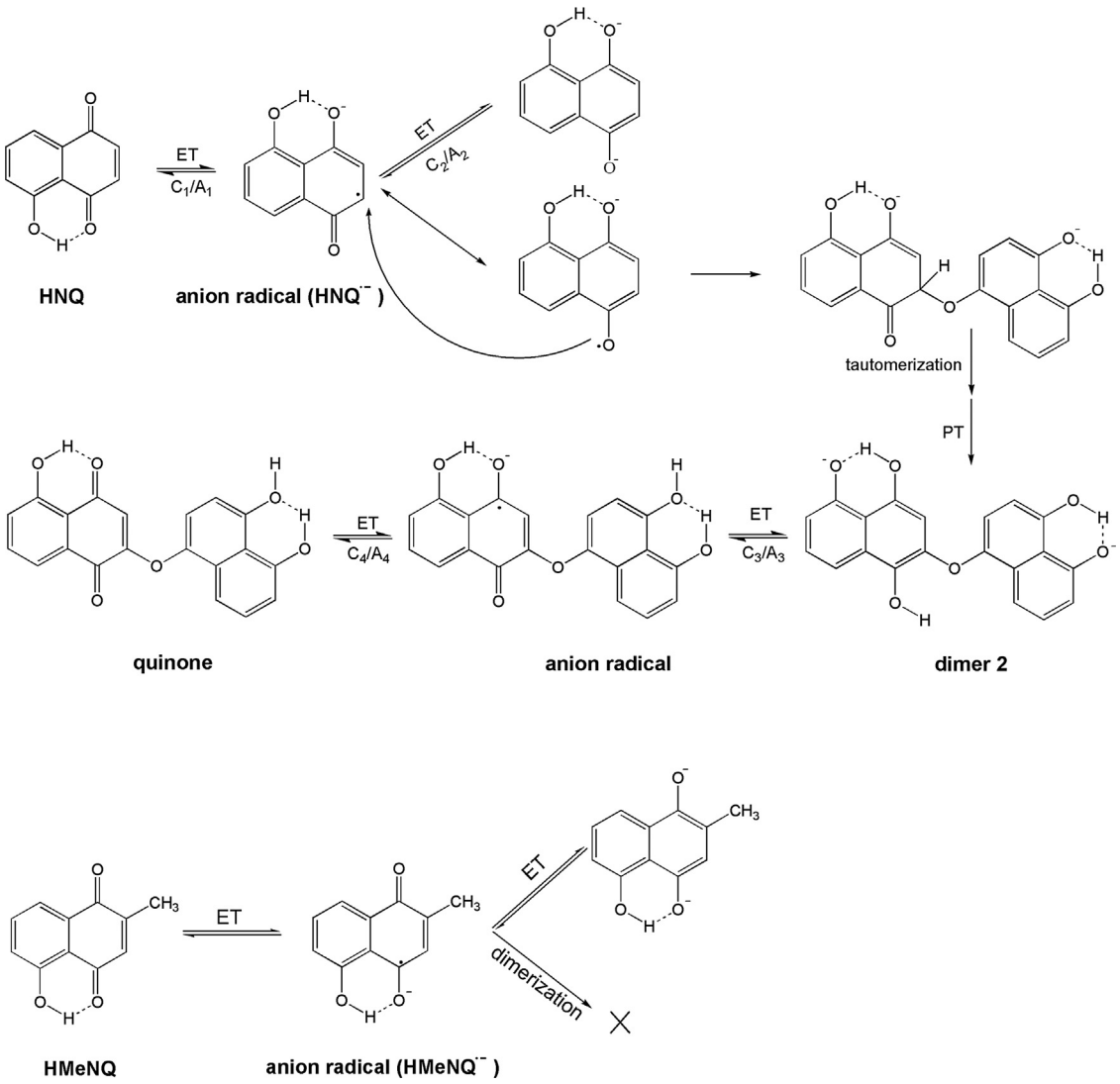

Scheme 3. Reduction process of HNQ and HMeNQ.

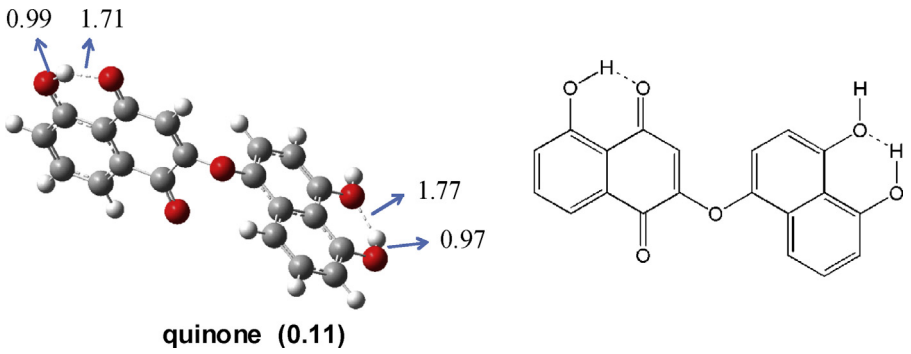

Fig. 13. Low–energy isomer for quinone at B3LYP/6-311++G** level and corresponding possible structure. The value in the brackets is relative energy in eV.

the second step. The relative energy of quinone is calculated and the result is listed in Fig. 13. It is 0.11 eV (relative to HNQ) in energy. Its possible structure is also in Fig. 13. Thus the whole reduction process of HNQ is shown in Scheme 3.

As discussed above, with concentration of proton donor increasing, intermolecular hydrogen–bonding between proton donor and $HNQ^{\bullet -}$ becomes more dominant. Oxidation of dimer is inhibited. Current value of C_4/A_4 and C_3/A_3 first decreases and then vanishes.

4. Conclusion

The electrochemical characteristics of HMeNQ and HNQ were studied by in situ FT-IR spectroelectrochemistry, CVA and DCVA. The results show that both HMeNQ and HNQ undergo two successive ET processes. However, HNQ should be explained with the help of the formation of dimer together. The current values related to dimer increase with added scan circles. The possible dimer structures are calculated at B3LYP/6-311++G** level, indicating PCET–accompanied C–centered and O–centered radical dimerization mechanism for HNQ. In addition, dimer also undergoes two successive ET processes to form quinone. With concentrations of added proton donor increasing, intermolecular hydrogen–bonding can block PCET and dimerization. The variation related to dimer in CV, CVA and DCVA first decreases and then vanishes.

Acknowledgment

This work has been supported by the National Nature Foundation of China (Grants 21175001 and 21273008), Doctoral Program Foundation of the Ministry of Education of China (20103401110001), the Foundation of Scientific Innovation Team of Anhui Province (2006KJ007TD), and the 211 Project of Anhui University.

References

[1] T.J. Monks, D.C. Jones, The metabolism and toxicity of quinones, quinonimines, quinone methides, and quinone-thioethers, Curr. Drug Metab. 3 (2002) 425.
[2] E. Katherine, W. Gary, Cytochrome b559 and cyclic electron transfer within photosystem II, Biochim. Biophys. Acta 1817 (2012) 66.
[3] P.N. Refojo, M. Teixeira, M.M. Pereira, The Alternative complex III: Properties and possible mechanisms for electron transfer and energy conservation, Biochim. Biophys. Acta 1817 (2012) 1852.
[4] T.M. Alligrant, J.C. Hackett, J.C. Alvarez, Acid/base and hydrogen bonding effects on the proton-coupled electron transfer of quinones and hydroquinones in acetonitrile: Mechanistic investigation by voltammetry,< sup>1</sup> H NMR and computation, Electrochim. Acta 55 (2010) 6507.
[5] D.R. Weinberg, C.J. Gagliardi, J.F. Hull, C.F. Murphy, C.A. Kent, B.C. Westlake, A. Paul, D.H. Ess, D.G. McCafferty, T.J. Meyer, Proton-coupled electron transfer, Chem. Rev. 112 (2012) 4016.
[6] P.D. Astudillo, D.P. Valencia, M.A. González-Fuentes, B.R. Díaz-Sánchez, C. Frontana, F.J. González, Electrochemical and chemical formation of a low-barrier proton transfer complex between the quinone dianion and hydroquinone, Electrochim. Acta 81 (2012) 197.
[7] L.A. Clare, L.E. Rojas-Sligh, S.M. Maciejewski, K. Kangas, J.E. Woods, L.J. Deiner, A. Cooksy, D.K. Smith, The Effect of H-Bonding and Proton Transfer on the Voltammetry of 2, 3, 5, 6-Tetramethyl-p-phenylenediamine in Acetonitrile. An Unexpectedly Complex Mechanism for a Simple Redox Couple, J. Phys. Chem. C 114 (2010) 8938.
[8] B. Jin, J. Huang, A. Zhao, S. Zhang, Y. Tian, J. Yang, Direct evidence of hydrogen-bonding and/or protonation effect on p-benzoquinone electrochemical reduction by in situ IR spectroelectrochemical study, J. Electroanal. Chem. 650 (2010) 116.
[9] Y.O. Kim, Y.M. Jung, S.B. Kim, S.M. Park, Two-dimensional correlation analysis of spectroelectrochemical data for p-benzoquinone reduction in acetonitrile, Anal. Chem. 76 (2004) 5236.
[10] G. March, S. Reisberg, B. Piro, M.-C. Pham, M. Delamar, V. Noel, K. Odenthal, D. Hibbert, J. Gooding, Electrochemical kinetic analysis of a 1, 4-hydroxynaphthoquinone self-assembled monolayer, J. Electroanal. Chem. 622 (2008) 37.
[11] M. Quan, D. Sanchez, M.F. Wasylkiw, D.K. Smith, Voltammetry of quinones in unbuffered aqueous solution: reassessing the roles of proton transfer and hydrogen bonding in the aqueous electrochemistry of quinones, J. Am. Chem. Soc. 129 (2007) 12847.
[12] P.D. Astudillo Sánchez, D.H. Evans, Reversible dimerization of the anion radicals of some dicyanonaphthalenes, J. Electroanal. Chem. 660 (2011) 91.
[13] A.B. Nepomnyashchii, M. Bröring, J. Ahrens, A.J. Bard, Chemical and Electrochemical Dimerization of BODIPY Compounds: Electrogenerated Chemiluminescent Detection of Dimer Formation, J. Am. Chem. Soc. 133 (2011) 19498.
[14] F. Teplý, M. Cížková, P. Slavíček, V. Kolivoška, J.n. Tarábek, M.n. Hromadová, L.r. Pospíšil, Electron Transfer Triggers Fast Dimer/Monomer Switching of Pyridinium and Quinolinium Cations, J. Phys. Chem. C 116 (2012) 3779.
[15] N.A. Maci´as-Ruvalcaba, G.A. Felton, D.H. Evans, Contrasting behavior in the reduction of 1, 2-acenaphthylenedione and 1, 2-aceanthrylenedione. Two types of reversible dimerization of anion radicals, J. Phys. Chem. C 113 (2009) 338.
[16] G. Armendáriz-Vidales, E. Martínez-González, H.J. Cuevas-Fernández, D.O. Fernández-Campos, R.C. Burgos-Castillo, C. Frontana, The Stabilizing role of Intramolecular Hydrogen Bonding in Disubstituted Hydroxy-Quinones, Electrochim. Acta 110 (2013) 628.
[17] G. March, S. Reisberg, B. Piro, M.C. Pham, C. Fave, V. Noel, Hydroxynaphthoquinone Ultrathin Films Obtained by Diazonium Electroreduction: Toward Design of Biosensitive Electroactive Interfaces, Anal. Chem. 82 (2010) 3523.
[18] W. Cheng, B. Jin, P. Huang, L. Cheng, S. Zhang, Y. Tian, Investigation on π-dimer/σ-dimer of 1, 8-Dihydroxy-9, 10-Anthracenedione in the process of Electrochemical reduction by Using IR Spectroelectrochemical Cyclic Voltabsorptometry and Derivative Cyclic Voltabsorptometry, J. Phys. Chem. C 117 (2013) 3940.
[19] N.A. Maci´as-Ruvalcaba, D.H. Evans, Association Reactions of the Anion Radicals of Some Hydroxyquinones: Evidence for Formation of π-and σ-Dimers As Well As a Neutral- Anion Radical Complex, J. Phys. Chem. C 114 (2010) 1285.
[20] J. Stubbe, W.A. van der Donk, Protein radicals in enzyme catalysis, Chem. Rev. 98 (1998) 705.
[21] J. Stubbe, D.G. Nocera, C.S. Yee, M.C. Chang, Radical initiation in the class I ribonucleotide reductase: long-range proton-coupled electron transfer? Chem. Rev. 103 (2003) 2167.
[22] C. Costentin, Electrochemical approach to the mechanistic study of proton-coupled electron transfer, Chem. Rev. 108 (2008) 2145.
[23] S.A. Poteet, M.B. Majewski, Z.S. Breitbach, C.A. Griffith, S. Singh, D.W. Armstrong, M.O. Wolf, F.M. MacDonnell, Cleavage of DNA by Proton-Coupled Electron Transfer to a Photoexcited, Hydrated Ru (II) 1, 10-Phenanthroline-5, 6-dione Complex, J. Am. Chem. Soc. 135 (2013) 2419.
[24] N. Song, C.J. Gagliardi, R.A. Binstead, M.-T. Zhang, H. Thorp, T.J. Meyer, Role of Proton-Coupled Electron Transfer in the Redox Interconversion between Benzoquinone and Hydroquinone, J. Am. Chem. Soc. 134 (2012) 18538.
[25] C. Costentin, M. Robert, J.M. Savéant, Electrochemical and homogeneous proton-coupled electron transfers: Concerted pathways in the one-electron oxidation of a phenol coupled with an intramolecular amine-driven proton transfer, J. Am. Chem. Soc. 128 (2006) 4552.

[26] J.M. Savéant, Electrochemical approach to proton-coupled electron transfers: recent advances, Energy Environ. Sci. 5 (2012) 7718.
[27] B. Jin, L. Li, J. Huang, S. Zhang, Y. Tian, J. Yang, IR spectroelectrochemical cyclic voltabsorptometry and derivative cyclic voltabsorptometry, Anal. Chem. 81 (2009) 4476.
[28] X. Wang, B. Jin, X. Lin, In-situ FTIR spectroelectrochemical study of dopamine at a glassy carbon electrode in a neutral solution, Anal. Sci. 18 (2002) 931.
[29] M.J. Frisch, G.W. Trucks, H.B. Schlegel, G.E. Scuseria, M.A. Robb, J.R. Cheeseman, G. Scalmani, V. Barone, B. Mennucci, G.A. Petersson, H. Nakatsuji, M. Caricato, X. Li, H.P. Hratchian, A.F. Izmaylov, J. Bloino, G. Zheng, J.L. Sonnenberg, M. Hada, M. Ehara, K. Toyota, R. Fukuda, J. Hasegawa, M. Ishida, T. Nakajima, Y. Honda, O. Kitao, H. Nakai, T. Vreven, J. Montgomery, J. A., J.E. Peralta, F. Ogliaro, M. Bearpark, J.J. Heyd, E. Brothers, K.N. Kudin, V.N. Staroverov, R. Kobayashi, J. Normand, K. Raghavachari, A. Rendell, J.C. Burant, S.S. Iyengar, J. Tomasi, M. Cossi, N. Rega, J.M. Millam, M. Klene, J.E. Knox, J.B. Cross, V. Bakken, C. Adamo, J. Jaramillo, R. Gomperts, R.E. Stratmann, O. Yazyev, A.J. Austin, R. Cammi, C. Pomelli, J.W. Ochterski, R.L. Martin, K. Morokuma, V.G. Zakrzewski, G.A. Voth, P. Salvador, J.J. Dannenberg, S. Dapprich, A.D. Daniels, O. Farkas, J.B. Foresman, J.V. Ortiz, J. Cioslowski, D.J. Fox, Gaussian 09, Revision B. 01,(2009), in, Gaussian, Inc., Wallingford CT, 2009.
[30] Y. Astuti, E. Topoglidis, P.B. Briscoe, A. Fantuzzi, G. Gilardi, J.R. Durrant, Proton-coupled electron transfer of flavodoxin immobilized on nanostructured tin dioxide electrodes: Thermodynamics versus kinetics control of protein redox function, J. Am. Chem. Soc. 126 (2004) 8001.
[31] N. Gupta, H. Linschitz, Hydrogen-bonding and protonation effects in electrochemistry of quinones in aprotic solvents, J. Am. Chem. Soc. 119 (1997) 6384.
[32] D. Tian, B. Jin, FT-IR spectroelectrochemical study of the reduction of 1, 4-dinitrobenzene on Au electrode: Hydrogen bonding and protonation in proton donor mixed media, Electrochim. Acta 56 (2011) 9144.